Electrode Energy Transfer Mechanisms in a MPD Arc

K. T. SHIH*
Convair Division of General Dynamics, San Diego, Calif.

AND

E. PFENDER†
University of Minnesota, Minneapolis, Minn.

A segmented anode is used for the confirmation of a proposed energy transfer model and for the measurements of circumferential current and heat flux distributions of a magnetoplasmadynamic arc. Two arc modes are observed; a mode with an asymmetric but steady-state current distribution and a mode with a rotating current spoke. The former occurs preferentially at higher gas injection velocities. There is no continuous transition between these two modes. By applying the experimental results to the anode energy transfer model, the contribution of the various energy transfer mechanisms to the observed anode energy fluxes can be determined. The energy flux due to the electron current is found to be the dominant mechanism. The net energy transfer to the cathode is much smaller than that to the anode, amounting to a few per cent only in an over-all energy balance.

Nomenclature

A = area, cm²
B = magnetic field strength, gauss
c_p = specific heat of gas at constant pressure, kjoules/kg-°K
e = electron charge, amp-sec
h = heat-transfer coefficient based on enthalpy difference, g/cm²-sec
i = enthalpy, kjoules/kg
I = current, amp
k = Boltzmann constant, kjoules/°K
$\dot{m}$ = mass flow rate, g/sec
Nu = Nusselt number
P = chamber pressure, mmHg
Q_A = total heat transfer to anode, kw
Q_C = total heat transfer to cathode, kw
Q_{CR} = heat transfer to anode by convection and radiation, kw
Q_G = heat transfer to the gas, kw
T = temperature, °K
U = arc voltage, v
U_a = anode fall, v
U_A = defined by Eq. (7), v
U_c = cathode fall, v
U_C = defined by Eq. (7), v
U_{CR} = defined by Eq. (7), v
U_G = defined by Eq. (7), v
U_I = defined by Eq. (4), v
η = thermal efficiency, %
κ = thermal conductivity, kw/cm-°K
ϕ = work function, v
χ = ionization potential, v

Subscripts

a = anode surface
c = cathode surface
e = electron
i = ion
s = plasma stream or anode segment
r = radiative

Received March 27, 1969; revision received August 1, 1969. This work was partially supported by NASA under Contract NAS 3-2595.

* Senior Research Engineer, Sensor Technology. Member AIAA.

† Professor, Heat Transfer Laboratory, School of Mechanical and Aerospace Engineering. Member AIAA.

Introduction

MANY efforts have been reported in recent years devoted to the development of a magnetoplasmadynamic (MPD) arc thruster for space missions.[1] Recent endeavors directed toward understanding the performance capacities of such thrusters stressed the need for a study of the mechanisms of electrode energy losses.

Based on the present understanding of electric arcs,[2,3] an energy balance at the electrode surfaces (Fig. 1) may be written by considering heat transfer by convection, radiation, and by electrons and/or ions carrying the electric current;

$$Q_A = h_a A_a(i_s - i_a) + Q_{ra} + I(5kT_e/2e + U_a + \phi_a) \quad (1)$$

$$Q_C = h_c A_c(i_s - i_c) - Q_{rc} + I_i(5kT_i/2e + \chi + U_c) - I\phi_c \quad (2)$$

In these simplified energy transfer equations, the following assumptions have been made. 1) The thermal accommodation coefficient for ions at the cathode shall be unity. 2) Q_{ra} and Q_{rc} represent the net absorbed or emitted radiation power at anode and cathode, respectively. 3) ϕ_a and ϕ_c are the effective work functions of anode and cathode, respectively. 4) ablation, sputtering, reflection of electrons, and secondary emission are neglected. The true electron temperature in Eq. (1) will be either close to the anode surface temperature or the freestream temperature, depending on whether or not

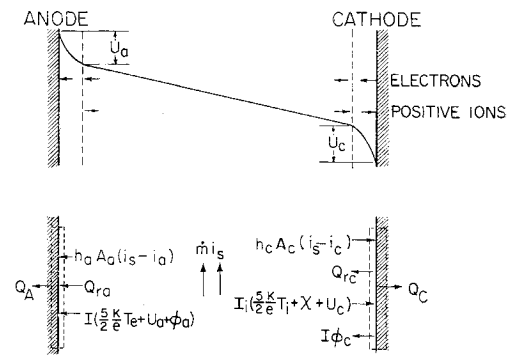

Fig. 1 Potential distribution and electrode energy balance of an electric arc.

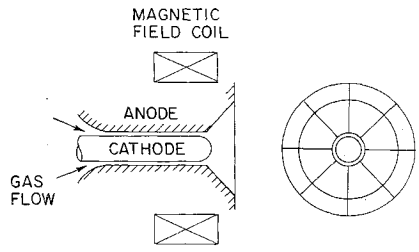

Fig. 2 Schematic of MPD arc thruster.

thermal equilibrium prevails in the boundary layer. Because of the relatively small number of collisions that the electrons suffer in the boundary layer, it is frequently argued that the electron temperature is close to the freestream temperature.

In this paper, the emphasis is on anode heat-transfer studies, because cathode losses are much smaller than those of the anode. In the proposed heat-transfer model as described by Eq. (1), the contribution of the electric current to the anode heat flux is separated from other heat-transfer mechanisms. The experimental work follows the same pattern using a segmented anode for separating these mechanisms, at the same time the segmentation allows to measure the circumferential current and heat flux distributions resolved according to the number of segments.

Experimental Apparatus

The anode and cathode assembly shown schematically in Fig. 2 is operated in an arc-tunnel as described in Ref. 4. Anode segmentation is illustrated in Fig. 3. The eight segments are each isolated both electrically and thermally from adjacent segments by a 10-mil-thick insulating paper. In addition, all segments have been relieved approximately 0.025 cm on their adjoining surface so that only a small rim around the edges actually touches the insulating paper, leaving a space between segments that further decreases the heat exchange. The current lead for each segment is brought out through a connecting bolt at the base of each segment. Each segment is made of copper and has water passages drilled in it; the water flow is connected in series. Thermocouples are located at the inlet of the first and the outlet of all segments to measure the temperature rise of the cooling water for calorimetric purposes. The inside diameter of the anode orifice is 1.27 cm. The cathode is made of thoriated (2%) tungsten having a diameter of 0.95 cm.

Experimental Results

Experiments have been conducted with the segmented anode in two different ranges of chamber pressures, using argon as working fluid. Stable arc operation is possible in the higher (above 20 mmHg) as well as in the lower range (below 1 mmHg), but the arc is unstable between these two ranges, and no reproducible data can be reported. The lowest pressure is limited to approximately 0.1 mmHg by the capacity of the existing vacuum equipment.

Experimental evidence shows that the effects of the ambient pressure on electrode heat transfer are insignificant. Hence,

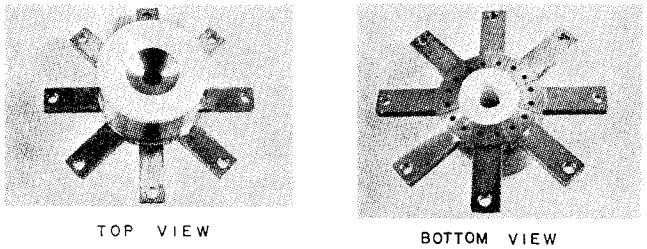

Fig. 3 Photographs of the segmented anode.

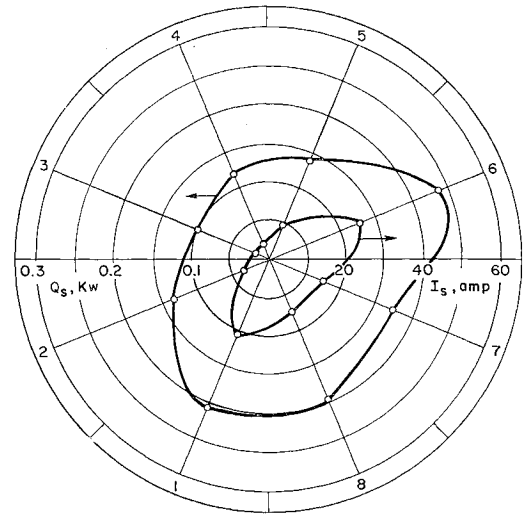

Fig. 4 Current and heat flux distributions; argon, I = 100 amp, P = 30 mmHg, m = 0.9 g/sec, B = 0.

the application of the results of this work, as discussed later in more detail, is warranted for actual MPD arcs that operate at much lower ambient pressure (less than 10^{-3} mmHg). A check of the arc characteristics using the segmented anode against characteristics obtained with a solid anode does not reveal a detectable difference.

A. Current and Heat Flux Distribution

Two different modes of current distribution have been observed. The heat-transfer data reported in this paper refer to a steady, but nonuniform current distribution to all eight segments. A typical case of such a current distribution with the associated heat flux distribution is shown in Fig. 4. The two distributions show a certain degree of similarity. Furthermore, the distributions do not change their general pattern of asymmetry at lower chamber pressure and/or with an applied magnetic field strength up to 2000 gauss.

Another mode with a rotating current spoke[5–7] was observed only at a mass flow rate below 40 mg/sec using an enlarged diameter of the anode orifice of 1.90 cm. These rotating current spokes were measured with conventional Rogowski coils wound around the segmental current leads. The change in anode geometry and flow rate results in a reduced gas velocity in the annular gap between the electrodes. Higher gas velocities probably blow the arc farther downstream, where the $j \times B$ interaction is weaker. This may be one reason why the arc does not rotate under these conditions. No quantitative measurements have been undertaken to confirm this conjecture. Qualitative observations at "spoke mode" are in agreement with those reported by other investigators.[5–7] It was also found that there is no continuous transition from the rotating to the nonrotating mode. At certain parameter settings, the arc may, indeed, shift back and forth between the two modes.

B. Identifying Anode Heat-Transfer Mechanisms

With the definition

$$Q_{CR} = h_a A_a (i_s - i_a) + Q_{ra} \tag{3}$$

and

$$U_I = 5kT_e/2e + U_a + \phi_a \tag{4}$$

Eq. (1) reduces to

$$Q_A = Q_{CR} + IU_I \tag{5}$$

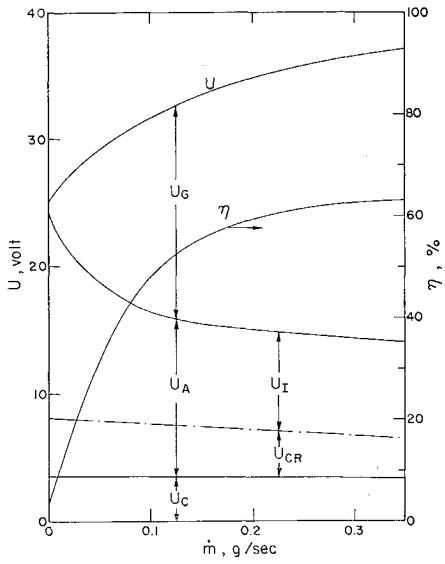

Fig. 5 MPD arc energy balance; argon, I = 100 amp, P = 20 mmHg, B = 0.

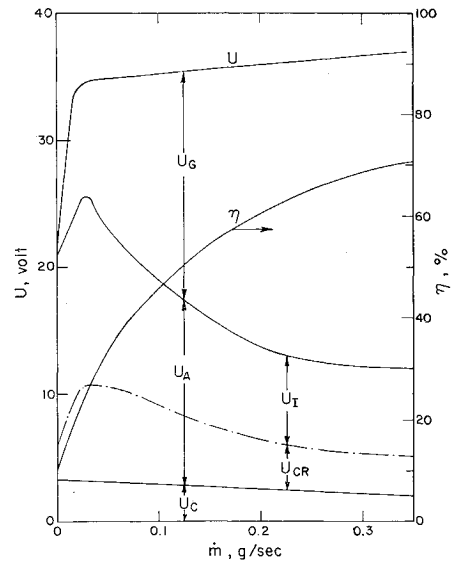

Fig. 6 MPD arc energy balance; argon, I = 200 amp, P = 20 mmHg, B = 0.

The first term on the right side of Eq. (5) is certainly not independent of the current because the plasma enthalpy and the associated convective heat transfer are current dependent. The same is true for the radiative heat flux received by the anode. This fact follows also from a comparison of the values of $U_{CR} = Q_{CR}/I$ plotted in Figs. 5 and 6 for two different arc currents, which indicates that there is an increase of Q_{CR} with increasing current. In general, U_I may also be a function of the current since the anode fall as well as the electron temperature may depend on the arc current, whereas ϕ_a is a constant for a given anode material. Therefore, any attempt to verify the anode heat-transfer model according to Eq. (5) by varying the total arc current requires that the dependence of Q_{CR} and U_I on the current be known.

In this paper another approach is applied which eliminates the current dependence of Q_{CR} by keeping the total arc current constant and varying segmental currents only. This approach implies that Q_{CR} is a function of the total current only, and does not depend on the current distribution. This is true for the radiative portion of Q_{CR} which stems essentially from the glowing cathode. Since the current distribution may influence local values of the film heat-transfer coefficient and of the enthalpy, it is not obvious that the convective part of Q_{CR} should be independent of the current distribution. Experimental evidence shows, however, that for the parameter range covered in this paper variations of Q_{CR} received by individual segments, if they exist, are small and may be neglected within experimental accuracy. Also, the sum of these individual heat fluxes remains constant as long as the total current is fixed.

The value of U_I evaluated for an individual segment depends on local values of electron temperature and anode fall. Recent Langmuir probe measurements close to the anode surface taken in the same arc configuration indicate that neither the electron temperature nor the anode fall shows a clear trend with varying current and the ensuing values of U_I are almost constant taking experimental accuracies into account.[8] Table 1, taken from Ref. 8 for comparable mass flow rates or pressures, indicates the variation of these parameters.

Table 1 Langmuir probe measurements

I, amp	$\dot{m}$, g/sec	P mmHg	U_e 10^3 °K	U_a, v	U_I, v
100	0.355	40	9	1.5	7.9
150	0.355	0.3	7.5	2.1	8.2
100	0.355	0.7	11.5	0.8	7.0
150	0.464	0.4	7.5	1.6	7.7
150	0.252	0.23	10	1.7	8.3

Based on these results, it is assumed in this study that U_I in a first-order approximation is independent of the current.

The anode heat-transfer model which predicts now a linear relationship between Q_s and I_s is applicable to any individual anode segment, but it does not hold for situations in which the total arc current is varied unless Q_{CR} contributes very little to the anode energy transfer. The latter depends on the arc configuration and the arc parameters.

Simultaneously taken data of segmental currents, I_s, plotted versus segmental heat fluxes, Q_s, result in a straight line (Fig. 7). The slope of the straight line yields the value of U_I, and the intercept with the ordinate gives the average heat flux Q_{CR} per segment. Segmental currents are varied with a variable resistor inserted into one of the segmental current circuits. The current to this segment is then controlled by the resistor, which causes a readjustment of the entire distribution. Within experimental accuracy, plots of Q_s versus I_s for any individual segment show a straight line and yield the same values of Q_{CR} and U_I, confirming the proposed anode energy transfer model. Figure 7 contains values from all eight segments to demonstrate the scatter of the data. The relative uncertainties are much higher at small segmental currents as indicated in Fig. 7.

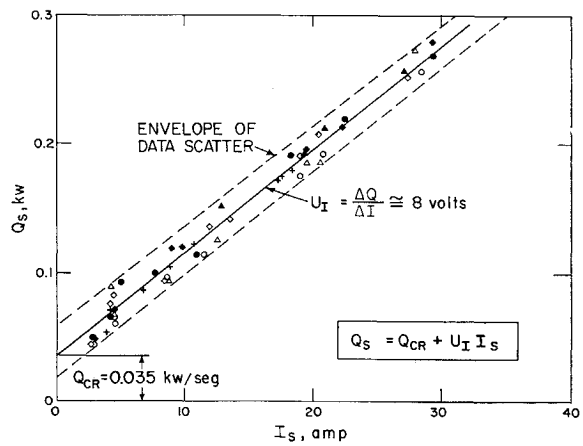

Fig. 7 Segmental heat fluxes versus current; argon, I = 100 amp, P = 30 mmHg, $\dot{m}$ = 0.218 g/sec, B = 0. Different symbols refer to different runs.

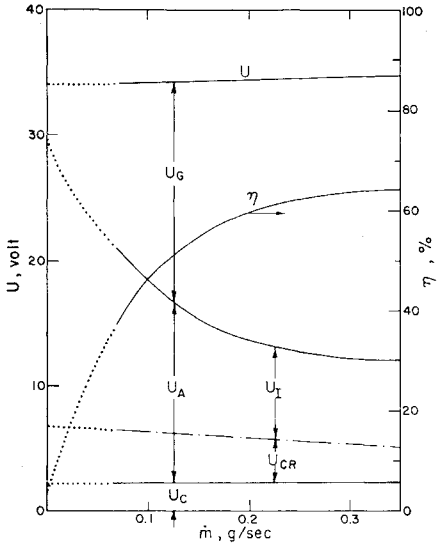

Fig. 8 MPD arc energy balance; argon, I = 200 amp, P ≤ 1 mmHg, B = 0; dotted lines are extrapolated.

C. Parametric Heat Balance Studies

For the following studies, the total power input and the heat flux into the anode and cathode are measured for different arc parameter settings. Further, heat fluxes into the anode are subdivided according to Eq. (5). For an over-all energy balance of the arc, the power input, IU, is compared with the sum of the heat fluxes to the anode, Q_A, to the cathode, Q_C, and to the gas, Q_G;

$$IU = Q_A + Q_C + Q_G \tag{6}$$

By introducing

$$U_A = Q_A/I, \quad U_C = Q_C/I, \quad U_{CR} = Q_{CR}/I, \quad U_G = Q_G/I \tag{7}$$

and substituting Eq. (5) into Eq. (6), one obtains

$$U = U_G + U_I + U_{CR} + U_C \tag{8}$$

In addition, the thermal efficiency is defined as

$$\eta = U_G/U \tag{9}$$

Figures 5,6 and 8–10 show data according to Eq. (8), which represents a total energy balance in terms of a voltage balance. The corresponding energy fluxes may be obtained by multiplying the voltage in these plots with the specified current.

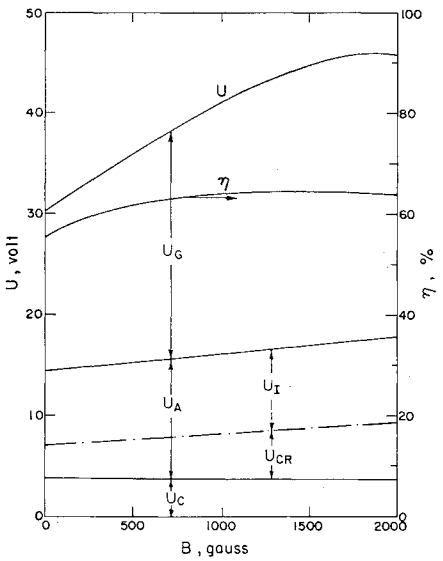

Fig. 9 Effect of magnetic field strength on energy balance; argon, I = 100 amp, P = 30 mmHg, ṁ = 1.1 g/sec.

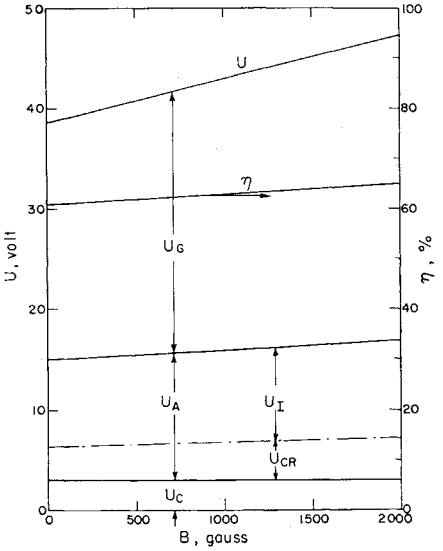

Fig. 10 Effect of magnetic field strength on energy balance; argon, I = 150 amp, P = 0.2 mmHg, $\dot{m}$ = 0.116 g/sec.

All quantities in Fig. 5 show some dependence on the mass flow rate. The arc voltage is the sum of anode fall, cathode fall, and electrical field strength integrated over the length of the arc column. Probably neither anode nor cathode fall is strongly influenced by the mass flow rate, because the thickness of the sheath in front of the electrodes is normally only of the order of one mean-free-path length, which is much thinner than the boundary-layer thickness. Therefore, the conditions within the sheath should be effectively protected from the flowfield by the boundary layer. There may be, however, some secondary effects of the electrode falls, such as property changes in the arc column, changes of the upstream pressure, etc. The electrical field strength, as well as the length of the arc column, will increase with increasing mass flow rate. The former is caused by greater energy exchange between plasma column and gas flow, whereas the latter is due to arc flow interactions.[9]

According to Eq. (4), three quantities may influence the value of U_I: electron temperature, anode fall, and the work function of the anode material. Since ϕ_a does not vary with mass flow rate (for copper $\phi_a \approx 4.47$ v),[10] the electron temperature and/or the anode fall would have to decrease with increasing mass flow. By means of a simple analytical model, Sherman and Yeh[11] have shown that the electron temperature decreases with increasing mass flow rate, which is consistent with the results of this study. The effects of mass flow rate on anode fall are still unknown, although in the previous paragraph it is argued that it will not be strongly affected.

U_{CR}, as defined by Eqs. (3) and (7), include the convective and radiative part of the anode heat transfer. The convective part, $h_a A_a (i_s - i_a)$, can be roughly estimated by assuming $Nu = h_a C_p d/\kappa = 3.65$,[12] $A_a = 2\text{cm}^2$, where $i_s = IU_G/\dot{m}$, $i_a = 520$ kjoules/kg (corresponding to an anode surface temperature of 1000°K). In comparison to measured values of U_{CR}, the calculated convective heat flux seems to be in the right order of magnitude. Three different types of radiation heat-transfer processes may occur at the anode surface: plasma to anode, anode to surroundings, and cathode to anode. The first two are small and may be neglected.[13] At low pressures, a large portion of the cathode is heated by the arc so that a certain amount of energy will be radiated from the cathode to the anode. By considering a process of combined conduction and radiation, an analytic solution of the energy equation of the present cathode geometry shows that an energy of the order of 0.5 kw is emitted from the cathode surface, assuming a tip temperature of 3000°K.

With the present experimental arrangement, a parametric study of the cathode heat balance is rather difficult. Because

of the minor importance of cathode losses, there has been no attempt to make such measurements. Figure 5 shows a small decrease of U_C with increasing mass flow rate.

The thermal efficiency depends strongly on the mass flow rate, and is very low at small mass flow rates—one reason for the low over-all efficiencies of MPD arc thrusters.

Data of Fig. 6, taken with a total current of 200 amp, show a peculiar maximum of U_I at small mass flow rates—which coincides with a sudden change of the arc voltage gradient. Visually, the arc jet increases its luminosity as though the anode arc attachment moved farther downstream.

Data in Fig. 8 refer to the low-pressure range ($P \leq 1$ mmHg). The chamber pressures are now a function of the mass flow rate. The general trend of the quantities, U_G, U_I, U_{CR}, and U_C is the same as before; the arc voltage, however, is almost independent of the mass flow rate. At a mass flow rate of $\dot{m} \leq 70$ mg/sec, the arc becomes unstable and extinguishes with the chosen parameters. The similarity to the results in Fig. 6 beyond 70 mg/sec flow rate suggests that a similar arc condition prevailed in spite of the different ambient pressures. Measurements of the pressures upstream of the anode orifice show that the back pressures are about the same in both cases (35 to 50 mmHg, depending on mass flow rate). Since the majority of the current attaches to the anode close to the orifice,[14] the arc is in both cases operated in the same pressure environment, so that arc voltage and electrode heat transfer are governed by the back pressure rather than the ambient pressure.

Figures 9 and 10 show the effect of the magnetic field strength on the quantities contained in Eq. (8). The arc voltage increases with increasing magnetic field strength. Patrick and Schneiderman[15] derived a linear relationship between the arc voltage and the superimposed magnetic field strength in a MPD arc. The data of this work support their theory in the low-pressure range (Fig. 10), but in the medium-pressure range (Fig. 9) deviations from the linear relationship occur.

U_C is essentially independent of B, whereas U_A increases slightly with increasing magnetic field strength. The small increase of U_{CR} with B may be caused by a somewhat higher convective heat transfer. There is also a small effect of the magnetic field on U_I; however, at this time, no conclusion can be drawn with regard to the individual changes of T_e and U_a. From Figs. 9 and 10, it follows that the magnetic field has a favorable influence upon the thermal efficiency, because the slope of the arc voltage versus the magnetic field strength is greater than the slope of U_A.

Conclusion

In this paper, the validity of a simple anode energy transfer model is demonstrated which is, in general, only applicable to a segmented anode. This model allows to determine the contribution of different mechanisms to the total heat flux. Under the present experimental conditions it is found that 70 to 80% of the anode heat flux is carried by the electric current. There is a strong dependence of the thermal efficiency on the mass flow rate. Considering the anode heat transfer only, it is undesirable to operate the arc at a very low mass flow rate. Applied magnetic fields have a small, but favorable influence on the thermal efficiency.

Two arc modes are observed under different operating conditions; an asymmetric, nonrotating current distribution and a rotating spoke. The latter is observed only at reduced mass flow rates and with enlarged anode orifices. The effects that the second arc mode may have on the anode heat transfer have not yet been studied. It is anticipated that a similar relationship between currents and anode heat fluxes may be established, based on time-averaged values.

References

[1] Nerheim, N. M. and Kelly, A. J., "A Critical Review of the State-of-the-Art of the MPD Thruster," AIAA Paper 67-688, Colorado Springs, Colo., 1967.

[2] Somerville, J. M., *The Electric Arc*, Methuen, London, 1959, Chap. 3.

[3] Finkelnburg, W. and Maecker, H., "Electric Arcs and Thermal Plasmas," *Handbuch der Physik*, Vol. XXII, Springer-Verlag, Berlin, 1956, pp. 254–444.

[4] Shih, K. T., Pfender, E., Ibele, W. E., and Eckert, E. R. G., "Experimental Anode Heat-Transfer Studies in a Coaxial Arc Configuration," *AIAA Journal*, Vol. 6, No. 8, Aug. 1968, pp. 1482–1487.

[5] Larson, A. V., "Experiments on Current Rotations in an MPD Engine," *AIAA Journal*, Vol. 6, No. 6, June 1968, pp. 1001–1006.

[6] Ekdahl, C., Kribel, R., and Lovberg, R., "Internal Measurements of Plasma Rotation in an MPD Arc," AIAA Paper 67-655, Colorado Springs, Colo., 1967.

[7] Connolly, D. J., Sovie, R. J., Michels, C. J., and Burkhart, J. A., "Low Environmental Pressure MPD Arc Tests," *AIAA Journal*, Vol. 6, No. 7, July 1968, pp. 1271–1276.

[8] Bose, T. K. and Pfender, E., "Direct and Indirect Measurements of the Anode Fall in a Coaxial Arc Configuration," *AIAA Journal*, Vol. 7, No. 8, Aug. 1969, pp. 1643–1645.

[9] Myers, T. W. and Roman, W. C., "Survey of Investigations of Electric Arc Interactions with Magnetic and Aerodynamic Fields," ARL 66-0184, Thermo-Mechanics Research Lab., Aerospace Research Labs., Dayton, Ohio, 1966.

[10] Gray, D. C., *American Institute of Physics Handbook*, 2nd ed., McGraw-Hill, New York, 1963, Sec. 9, p. 148.

[11] Sherman, A. and Yeh, H., "Blowing of Current Patterns in Nonequilibrium Plasma," *AIAA Journal*, Vol. 5, No. 9, Sept. 1967, pp. 1689–1690.

[12] Eckert, E. R. G. and Drake, R. M., Jr., *Heat and Mass Transfer*, McGraw-Hill, New York, 1969, p. 193.

[13] Schoeck, P. and Eckert, E. R. G., "An Investigation of Anode Heat Transfer in High Intensity Arcs," *Proceedings, Fifth International Conference in Ionization Phenomena in Gases, Munich*, North-Holland, Amsterdam, 1961, pp. 1812–1831.

[14] Powers, W. E., "Measurements of the Current Distribution in the Exhaust of an MPD Arcjet," *AIAA Journal*, Vol. 5, No. 3, March 1967, pp. 545–550.

[15] Patrick, R. M. and Schneiderman, A. M., "Performance Characteristics of a Magnetic Annular Arc," *Sixth Symposium on Engineering Aspects of Magnetohydrodynamics*, University of Pittsburgh, Pittsburgh, Pa., April 1965, pp. 70–77.